Eur Biophys J (1993) 22:169–175

European Biophysics Journal

Fluorescence correlation spectroscopy with high count rate and low background: analysis of translational diffusion

R. Rigler [1], **Ü. Mets** [1, 2], **J. Widengren** [1], **P. Kask** [2]

[1] Karolinska Institute, Department of Medical Biophysics, S-10401 Stockholm, Sweden
[2] Institute of Chemical Physics and Biophysics, Estonian Academy of Sciences, Rävala 10, EE-0001 Tallinn, Estonia

Received: 29 September 1992 / Accepted in revised form: 17 March 1993

Abstract. An epi-illuminated microscope configuration for use in fluorescence correlation spectroscopy in bulk solutions has been analyzed. For determining the effective sample dimensions the spatial distribution of the molecule detection efficiency has been computed and conditions for achieving quasi-cylindrical sample shape have been derived. Model experiments on translational diffusion of rhodamine 6G have been carried out using strong focusing of the laser beam, small pinhole size and an avalanche photodiode in single photon counting mode as the detector. A considerable decrease in background light intensity and measurement time has been observed. The background light is 40 times weaker than the fluorescence signal from one molecule of Rh6G, and the correlation function with signal-to-noise ratio of 150 can be collected in 1 second. The effect of the shape of the sample volume on the autocorrelation function has been discussed.

Key words: Fluorescence correlation spectroscopy – Fluorescence intensity fluctuations – Translational diffusion – Epifluorescence microscope – Silicon photon counter

1. Introduction

Fluorescence correlation spectroscopy (FCS) is a method for probing the kinetic properties of molecular systems. It possesses several unique qualities, including the ability to measure absolute concentrations (Elson and Magde 1974), extreme sensitivity, as well as the ability to measure rotational diffusion in time ranges much longer than the fluorescence lifetime of the probe (Ehrenberg and Rigler 1974). FCS has mainly been used in studies of translational diffusion of labelled macromolecules in solutions and membranes. Wider use of FCS has been hindered by the complexity of the experimental setup and by the length of data collection times needed to achieve acceptable a signal-to-noise ratio. An epi-illuminated microscope was first used in FCS by Koppel et al. (1976). The effect of the finite length of the sample volume on the measured autocorrelation function has been studied by Rigler and Widengren (1990). Qian and Elson (1991) have given a detailed analysis of light collection properties of a microscope with a pinhole in the image plane. The purpose of the present work is to clarify the problem of the sample shape in the epi-illuminated microscope which is important for precise measurement of translational diffusion in bulk solution.

Correspondence to: R. Rigler

2. Theoretical background

The intensity distibution in any cross-section of a laser beam in the fundamental mode is Gaussian. If we observe a parallel beam of this kind through a slit which has a Gaussian transmission profile in the direction of propagation of the beam, we get the so-called quasi-cylindrical profile of the observation volume. This profile can be described by a Gaussian distribution of the detected intensity:

$$I(x, y, z) = I_0 \exp\left(-2\frac{(x^2 + y^2)}{w_0^2}\right) \exp\left(-2\frac{z^2}{z_0^2}\right) \qquad (1)$$

where x, y and z are the coordinates of a fluorescent particle under the microscope objective and the laser beam propagates along the z-axis. For this profile Aragón and Pecora (1976) have derived the autocorrelation function of fluorescence intensity of diffusing particles:

$$G(t) = 1 + \frac{1}{N}\left(1 + \frac{4Dt}{w_0^2}\right)^{-1}\left(1 + \frac{4Dt}{z_0^2}\right)^{-1/2} \qquad (2)$$

where D is the translational diffusion coefficient, w_0 is the sample radius, $2z_0$ is the effective length of the sample and N is the average number of fluorescent molecules in the sample volume.

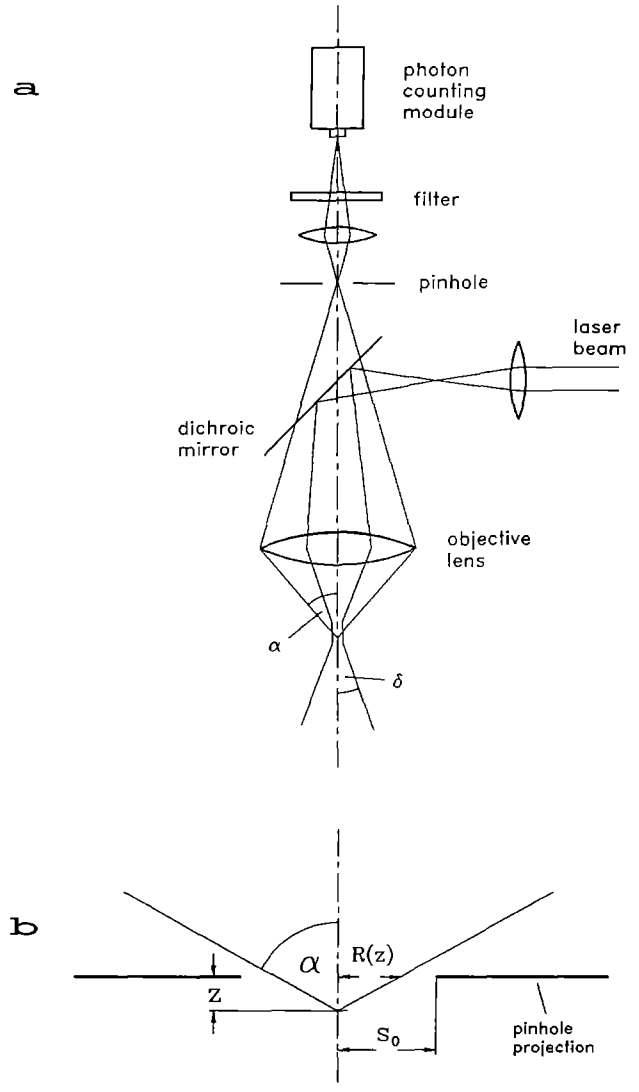

Fig. 1. **a** Schematic diagram of the epi-illuminated microscope with a pinhole in the image plane, **b** illustration of fluorescence collection under the objective. The size of the pinhole projection s_0 is equal to the physical size of the pinhole divided by the magnification of the objective. The size of the PSF $(\boldsymbol{r}, \boldsymbol{r}'\, z)$ is determined by the cross-section in the object plane of the cone of half-angle α with the top in the point $(\boldsymbol{r}', z)$. The CEF $(\boldsymbol{r}', z)$ is determined by the common area of the PSF $(\boldsymbol{r}', z)$ and the pinhole projection, normalized to the total area of the PSF

However, equation (1) is not the exact expression for the profile of the detected intensity in an epifluorescence microscope with the pinhole in the image plane. First of all, the radius of a focused laser beam is not a constant but a function of z. Secondly, the profile of the detected intensity along the optical axis is not exactly Gaussian. The reason for using expression (1) to model the real situation is that the autocorrelation function in an analytical form has not been derived for more complex intensity distributions. In the following we shall try to find out under which circumstances the profile (1) is adequate.

The exactness of the intensity profile in the z-direction is not very critical because it only affects the square root factor of the autocorrelation function (2), which is usually smooth because $z_0 > w_0$. Also, Elson and Magde (1974) have shown that the autocorrelation functions for Gaussian and rectangular excitation profiles are rather similar. Therefore we shall consider z_0 as an effective parameter. In order to justify the application of expression (1) we have to find the geometry of the optical system which results in practically constant radius of the sample volume. To achieve this we shall now analyze in some detail the light collection properties of the microscope and the profile of the excitation beam.

The effect of the pinhole in the image plane of a microscope (Fig. 1 a) can be described using the fluorescence collection efficiency function CEF $(\boldsymbol{r}', z)$ (Koppel et al. 1976). This function is defined as the fraction of light, emitted by a point source, that passes through the pinhole. Its value depends on the location and size of the image of the point source with respect to the pinhole. Following Qian and Elson (1991) we set magnification equal to 1, which is equivalent to projecting the pinhole into the sample space (Fig. 1 b). We represent the transmission function of the pinhole $T(\boldsymbol{r})$ by the disk function:

$$T(\boldsymbol{r}) = \mathrm{circ}\left(\frac{\boldsymbol{r}}{s_0}\right), \tag{3}$$

$$\mathrm{circ}\left(\frac{\boldsymbol{r}}{s_0}\right) = \begin{cases} 1 & \text{if } |\boldsymbol{r}| \le s_0 \\ 0 & \text{if } |\boldsymbol{r}| > s_0 \end{cases},$$

where s_0 is the radius of the pinhole projected to the sample space and $\boldsymbol{r}$ is the projection of the image plane radial coordinate.

The point spread function of the microscope describes the image of a point source, located at $(\boldsymbol{r}', z)$ in the sample, in terms of intensity distribution in the image plane. We also approximate this function by the disk function centered at $\boldsymbol{r}'$:

$$\mathrm{PSF}(\boldsymbol{r}, \boldsymbol{r}', z) = \frac{\mathrm{circ}\left(\dfrac{\boldsymbol{r} - \boldsymbol{r}'}{R(z)}\right)}{\pi R^2(z)}, \tag{4}$$

where $R^2(z) = R_0^2 + z^2 \tan^2 \alpha$.
$R(z)$ is the radius of the image spot of a point source located at distance z from the object plane,

$\boldsymbol{r}'$ is the radial coordinate of the point source in the sample space.
α is the aperture half-angle of the microscope objective and
R_0 is the resolution limit of the objective.

The collection efficiency function can be expressed as:

$$\mathrm{CEF}(\boldsymbol{r}', z) = \frac{1}{\Delta} \int T(\boldsymbol{r})\, \mathrm{PSF}(\boldsymbol{r}, \boldsymbol{r}', z)\, d\boldsymbol{r}, \tag{5}$$

where Δ is a normalization factor and the integral is taken over the image plane. Invariance of the point spread function with respect to translation perpendicular to the z-axis has been assumed here.

The radius of the focused laser beam $w(z)$ can be expressed as:

$$w^2(z) = w_0^2 + z^2 \tan^2 \delta, \tag{6}$$

where $w_0 = \dfrac{\lambda}{n\pi \tan\delta}$ is the beam waist radius at $1/e^2$ intensity,

δ is the focusing angle of the laser beam in the sample at $1/e^2$ intensity,
z is the distance from the object plane along the optical axis,
λ is the laser wavelength in vacuum,
n is the index of refraction of sample.

The intensity profile of this beam is Lorentzian along the z-axis and Gaussian in the radial direction:

$$I(r', z) = \frac{2P}{\pi w^2(z)} \exp\left(-2\frac{r'^2}{w^2(z)}\right), \tag{7}$$

where P is the power of the laser beam and $w^2(z)$ is given by expression (6).

3. Molecule detection efficiency calculations

We define the molecule detection efficiency (MDE) as the collection efficiency function multiplied by the excitation intensity:

$$\mathrm{MDE}(r', z) = \mathrm{CEF}(r', z) \cdot I(r', z). \tag{8}$$

This function, sometimes also called the apparent excitation profile, determines the dimensions of the effective sample volume in FCS, as it measures the detected relative intensities of fluorescence from a molecule under real illumination.

The principal independent parameters of the optical system are:

a) numerical aperture of the objective: $n \cdot \sin\alpha$,

b) pinhole radius, projected to the sample space: $s_0 = \dfrac{r_0}{M}$, where r_0 is the radius of the pinhole and M is the magnification of the objective,

c) focusing angle of the laser beam: δ.

Laser wavelength λ and the index of refraction of the sample n are taken as constants. Requiring a practically non-apertured Gaussian beam poses a restriction on the laser focusing angle: $\delta \leqslant \alpha/2$. Figure 2 presents an example of the distribution of the molecule detection efficiency and its factors: the laser beam intensity and the fluorescence collection efficiency. In Fig. 2b it can be seen that there is a plateau in the central part of the CEF (r', z). The light emitted from this part of the sample is not blocked by the pinhole. The light, emitted from the points on the z-axis corresponding to the edge of the plateau, precisely fills the pinhole (i.e. $R(z) = s_0$, see Fig. 1b). From analysis of different MDE plots we concluded that the radius of the sample volume is defined by the part of the laser beam between these corner points. For the points farther away from the object plane an increasing fraction of light is blocked by the pinhole. Allowing a maximal increment of 10% for the beam radius ($w(z) \leq 1.1\, w_0$) and using expressions (6) and (4) we estimate the upper limit for usable pinhole radius at a given focusing and numerical

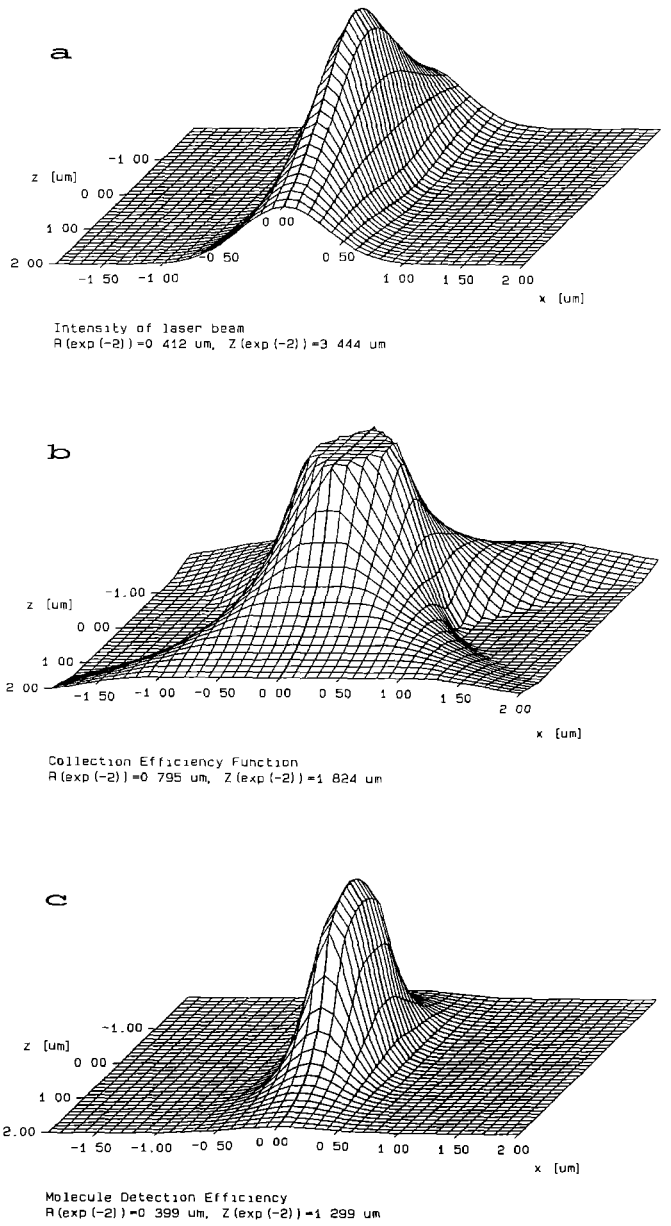

Fig. 2. Spatial distributions of **a** the intensity of the laser beam, **b** the collection efficiency function CEF (r', z), **c** the molecule detection efficiency MDE (r', z) for the 40×0.9 objective together with the pinhole of 25 μm radius and the laser focusing angle of 0.3 rad. The plot **c** is a point by point product of **a** and **b**. z is the axial coordinate, x is the radial coordinate

aperture of the objective:

$$s_{\max} = \frac{0.5 \tan\alpha}{\tan\delta} w_0. \tag{9}$$

The lower limit for the pinhole radius $s_{\min}$ equals the radius of the laser beam waist w_0. The sample radius is close to w_0 in both cases. If $s_0 > s_{\max}$ or $s_0 < s_{\min}$ then the variation in the sample radius exceeds the allowed limit and profile (1) is not valid with the required precision. From geometrical considerations it is possible to find the $1/e^2$ points of the collection efficiency CEF $(0, z)$ on the optical axis (see Fig. 1b). For these points the area of the point spread function PSF $(r, 0, z')$ is equal to e^2 times the

pinhole area, i.e. $R(z') = e s_0$ and the corresponding distance from the object plane is

$$z' = \frac{e s_0}{\tan \alpha}. \tag{10}$$

This value can be used as a crude estimate of the half-length of the sample in the z-direction. The correct $1/e^2$ point of MDE ($z = z_0$) is located at somewhat smaller z values because the laser intensity decreases with increasing z. This error is 28% for $\sin\alpha = 0.9$ and maximum s_0, and decreases to 1% if $s_0 = w_0$. For $\sin\alpha = 0.4$ the error is between 27% and 12%. We can also estimate the range of realizable length-to-diameter ratios of the quasi-cylindrical sample:

$$\frac{e}{\tan\alpha} \leq \frac{z_0}{w_0} \leq \frac{0.5\, e}{\tan\delta}, \tag{11}$$

keeping in mind that $\delta \leq \alpha/2$.

These simplified expressions for z_0 assume that we are far from the resolution limit of the objective $s_0 \gg R_0$. Otherwise we have to substitute $\sqrt{s_0^2 + R_0^2}$ for s_0. At large focusing angles and small pinhole sizes spherical aberrations also become significant and in practice z_0 cannot be made smaller that about 1 μm (Palmer and Thompson 1989; Schneider and Webb 1981).

4. Experimental

The experimental setup consists of a CW Ar^+ laser (Spectra Physics 165), an epi-illuminated microscope (Leitz), a semiconductor photon counting module consisting of a Peltier-cooled avalanche photo diode (EG&G Optoelectronics SPCM-100-PQ) and a correlator (Langley-Ford 1096). The laser is operated at 514.5 nm and 200 mW power to have good stability. Neutral glass filters are used to attenuate the laser power to 0.25–0.5 mW in the sample. The laser beam size in the sample is controlled by varying the beam size on the lens in front of the microscope. Two microscope objectives were used: 63×1.2 water immersion objective (Zeiss Plan-Neofluar) and 40×0.9 objective, adjustable to water, glycerol or oil immersion with or without the cover slip (Zeiss Plan-Neofluar). The laser beam is directed via a dichroic mirror and the microscope objective to the sample along the optical axis (Fig. 1 a). The fluorescence is focused by the same objective to the image plane, where a pinhole is located. The light passing through the pinhole is then focused onto the sensitive area of the avalanche photodiode in the photon counting module. Standard TTL pulses from the photon counting module are fed to the correlator. The autocorrelation curves from the correlator are transferred to a MicroVAX II computer. The data reduction program is based on a nonlinear least squares minimization algorithm (Marquardt 1963).

Translational diffusion of Rh6G (Lambdachrome, Lambda-Physik) at room temperature (22° C) was measured using the 40×0.9 and the 63×1.2 objectives in combinations with three different pinholes of 45 μm, 25 μm and 15 μm radii. The laser beam focusing angle as measured under the objective and corrected for the index of refraction of water was 0.33 rad with the 40×0.9 objective and 0.45 rad with the 63×1.2 objective. With these focusing angles the maximum pinhole radii according to expression (9) are 20 μm for the 40×0.9 objective and 35 μm for the 63×1.2 objective. Minimum allowed radius is about 15 μm for both objectives.

The detector was checked for self-correlations by measuring uniform light from a light-emitting diode. Up to the accuracy of 1 in 10000 there were no correlations in the micro- and millisecond time range except for the 200 ns dead time reported in the data sheet.

Table 1.

Objective	Pinhole radius [μm]	τ_{diff} [ms]	w_0 meas. [μm]	w_0 calc. [μm]	z_0 meas. [μm]	z_0 calc. [μm]	V meas. [fl]
40×0.9	45	0.213	0.489	0.361	8.0	1 71	12.0
	25	0.138	0.393	0.353	1.60	1.18	1.53
	15	0.091	0.320	0.298	1.53	0.80	0.984
63×1.2	45	0.089	0.316	0.256	1.74	0.61	0.716
	25	0.061	0.262	0.243	1.05	0.40	0.453
	15	0.041	0.213	0.209	0.85	0.28	0.242

5. Results and discussion

In our experiments we used rather strong focusing of the laser beam and correspondingly small pinhole sizes. The resulting small sample volume leads to increased fluctuation amplitudes at unchanged concentration and hence to improved signal-to-background ratio. Another advantage of the small sample volume is a shorter translational correlation time. This facilitates measurements on very large molecules and in very viscous environments. In the high counting rate situation, where the number of photocounts per molecule per counting interval is not much less that 1, the S/N ratio increases with square root of the ratio of the total counting time to the correlation time (Koppel 1974). The correlation curves were fitted with the autocorrelation function for translational diffusion (2). For comparison we also used the so-called 2-dimensional model, assuming $z_0 = \infty$:

$$G(t) = 1 + \frac{1}{N}\left(1 + \frac{4Dt}{w_0^2}\right)^{-1}.$$

Table 1 compares the sample dimensions calculated as the $1/e^2$ points of the MDE distribution (calc.) with those obtained by fitting the measured autocorrelation function with formula (2) (meas.) for various objective-pinhole combinations. The diffusion coefficient value of $D = 2.8 \times 10^{-6}\ cm^2\ s^{-1}$ has been used.

The correlation time τ_{diff} corresponds to the radial component of diffusion:

$$\tau_{diff} = \frac{w_0^2}{4D}.$$

Table 2.

Objective	Pinhole radius	3-*D* model		2-*D* model		change in τ_{diff}	increase in χ^2
	[μm]	τ_{diff} [μs]	χ^2	τ_{diff} [μs]	χ^2	[%]	[%]
40 × 0.9	45	213.7 ± 3.0	1.55	213.5 ± 3.0	1.50	0.1	−3.2
	25	137.9 ± 2.2	0.44	127.6 ± 3.4	1.65	7.5	275.0
	15	91.1 ± 2.0	0.72	88.1 ± 1.0	1.07	3.3	48.0
63 × 1.2	45	89.2 ± 1.0	0.87	87.8 ± 1.0	1.16	1.6	33.0
	25	61.2 ± 1.3	0.54	58.5 ± 1.7	1.98	4.5	267.0
	15	40.6 ± 0.7	0.49	37.6 ± 0.3	3.85	7.6	690.0

Table 3.

Pinhole radius	40 × 0.9 objective		63 × 1.2 objective	
[μm]	signal [s^{-1} molecule^{-1}]	background [s^{-1}]	signal [s^{-1} molecule^{-1}]	background [s^{-1}]
45	22000	22000	72000	14000
25	31000	8000	73000	3700
15	30000	3000	62000	1300

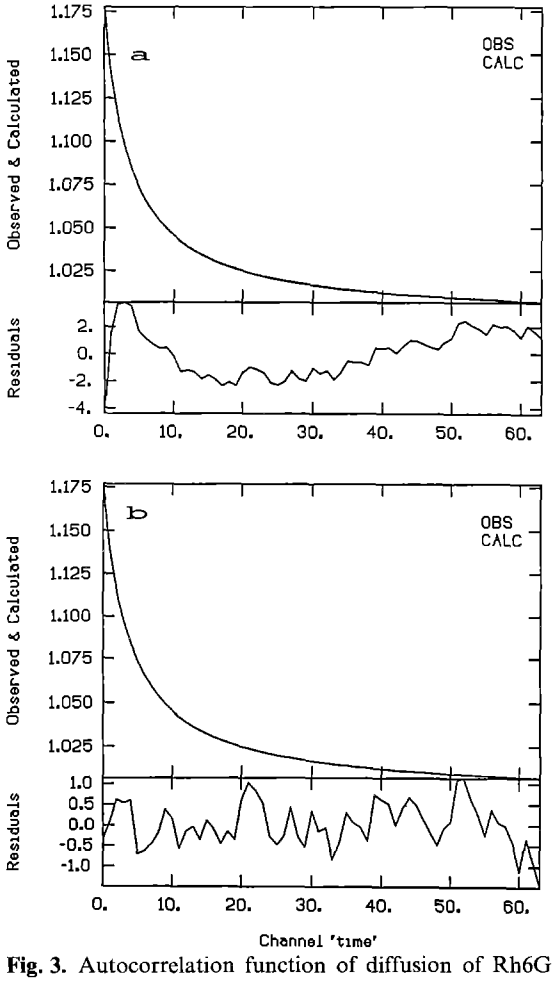

Fig. 3. Autocorrelation function of diffusion of Rh6G measured with the 63 × 1.2 objective and the pinhole of 15 μm radius. **a** fitted with the 2-*D* model, **b** fitted with the 3-*D* model. Duration of the measurement was 200 seconds

The measured and calculated values of w_0 coincide within 10% for the pinholes of 25 μm and 15 μm radii. The larger discrepancy with the 45 μm pinhole we attribute to the non-uniform sample radius, as in this case the radius of the pinhole projection s_0 exceeds the maximum value given by expression (9) and therefore profile (1) is not adequate. The measured axial dimension z_0 is in all cases considerably larger than the calculated value. For z_0 values of about 1 μm and less this discrepancy is caused by the spherical aberrations of the objective (Palmer and Thompson 1989; Schneider and Webb 1981).

Table 2 compares the measured radial correlation times which are obtained by fitting the same set of data with 2-*D* and 3-*D* models.

The χ^2 in this table is the normalized mean square deviation of the fitting curve from the measured correlation function. It is surprising to find χ^2 values below 1.0, indicating that the weighting function (Koppel 1974) overestimates the noise. The probable reason for this is that some of the assumptions (e.g. large number of molecules) made by Koppel (1974) are not fulfilled in our experiment. The confidence limits for the correlation time are standard deviations for a set of 4 to 6 measurements on the same solution.

From this table two conclusions can be drawn:

1. When using the 2-dimensional model instead of the more adequate 3-dimensional one, we do not make very large error in the estimated value of the correlation time. However, because of the larger χ^2 in case of the 2-*D* model the weakly manifested additional processes, if present, remain unrevealed. The difference in quality of fit is illustrated in Fig. 3.

2. With the 45 μm pinhole the difference in fit quality with different models is insignificant. This is because the assumption (1) is not valid in the case of the large pinhole and the fit with neither model is good.

The signal intensity data are collected in Table 3. The power of the laser beam in the sample was 0.25 mW.

It is interesting to note that the background intensity is approximately proportional to the square of the pinhole size. This means that the intensity of the background light in the image plane is practically uniform while the light from the sample is concentrated in the vicinity of the optical axis. This uniform light is probably the fluorescence of the objective, the dichroic mirror or the glass filter. Finding the origin of this light could reveal a way

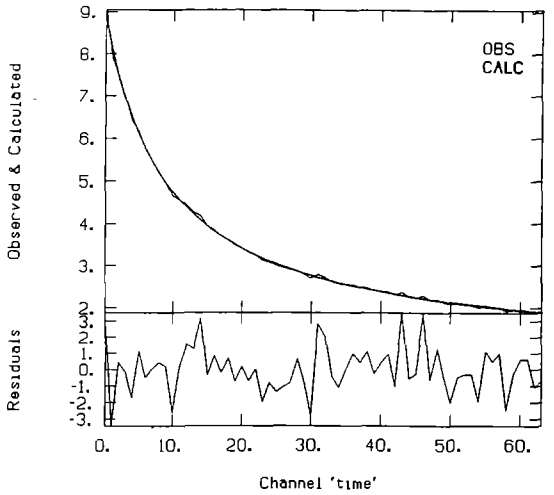

Fig. 4. Autocorrelation function of diffusion of Rh6G measured with the 63×1.2 objective and the pinhole of 15 μm radius. The average number of molecules in the sample volume $N = 0.025$. Duration of the experiment was 200 seconds

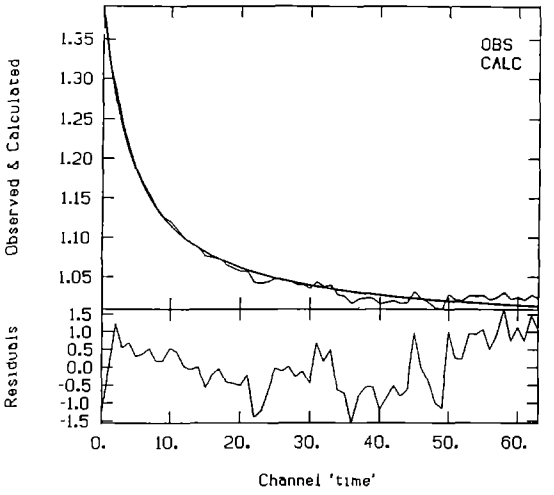

Fig. 5. Autocorrelation function of diffusion of Rh6G measured with the 63×1.2 objective and the pinhole of 15 μm radius (corresponding $s_0 = 0.24$ μm). Duration of the experiment was 200 milliseconds

of further improvement of the signal-to-background ratio. However, the value of background intensity with the 63×1.2 objective and the 15 μm pinhole was equal to 1/40 of the flourescence intensity of one Rh6G molecule which permitted us to do quite satisfactory experiments. One molecule per volume element (2×10^{-16} *l*) corresponds to a concentration of 0.7×10^{-8} *M* under these conditions. In Fig. 4 we present an autocorrelation function of Rh6G measured with the average number of molecules in the sample volume $N = 0.025$. The apparent number of molecules N_a is related to the actual number of molecules N and the background intensity N_b as $N_a = (N + N_b)^2/N$ (Koppel 1974). Here the background intensity N_b is expressed in equivalent number of fluorophore molecules. Figure 5 presents the autocorrelation function of diffusion of Rh6G, measured during 200 milliseconds.

The high speed of measurement facilitates new kinds of experiments, e.g. time-resolved diffusion measurements and measuring the spatial distribution of the diffusion coefficient using a scanning microscope.

The accuracy of determining the value of z_0 from the experiments is considerably lower than that of the other parameters. Fortunately z_0 and w_0 are constant for a given combination of the objective, the focusing angle of the laser beam, the laser wavelength and pinhole size. Consequently the ratio of the time constants in the autocorrelation function (2) is also constant. This ratio can be determined from a separate experiment with enhanced precision (e.g. a long measurement of Rh6G) and then introduced into the fitting function. So in routine measurements only one correlation time has to be fitted.

In contrast to Qian and Elson (1991) we have found that the sample profile in the properly arranged epifluorescence device can be modelled by 3-*D* Gaussian distribution (1) with excellent accuracy. With the 2-*D* model the deviations of the fitting function from the experimental data are larger, leading to reduced statistical accuracy of the obtained parameters.

The value of the correlation time obtained with the 2-*D* model is influenced by two phenomena in opposite directions. The finite sample length along the *z*-axis tends to reduce the correlation time of the 2-*D* model. The expansion of the laser beam size towards the ends of the sample volume leads to increased correlation times in both the 2-*D* and the 3-*D* model. In cases of lower signal-to-noise ratio or very long cylindrical sample profile the 2-*D* model can be used successfully, as the deviations are then hidden in the noise. Knowledge of the sample shape allows one to estimate the extent of systematic deviations from the model situation.

The exposure dose received by the diffusing fluorophores is independent of the beam radius w_0 (Koppel 1974) and so is the fraction of photobleached molecules in the beam. The light intensity is proportional to w_0^{-2} and by decreasing the beam size we come close to saturation of the excited state of fluorophores. With $w_0 = 0.24$ μm and 0.25 mW power of the laser beam the average lifetime of the ground state of Rh6G in the centre of the beam is about 4 ns, which is close to the excited state lifetime.

6. Conclusion

With properly chosen parameters of the optical system the 3-dimensional Gaussian distribution (1) describes the sample profile of the FCS experiment in an epifluorescence microscope with high accuracy. Owing to the high S/N ratio achieved via using the semiconductor photon counter and modified optics, it has been possible to determine the axial dimension of the sample volume from the measured autocorrelation function. The relatively high average number (about 4) of photocounts per molecule per average diffusion time for rhodamine 6G implies possibility of detecting individual molecules with our setup (Rigler et al. 1992; Rigler and Mets 1993).

Acknowledgements. We thank Prof. N. Åslund, Royal Institute of Technology for the loan of the avalanche photo diode and Per Thyberg for expert help in data communication. This investigation was supported by the Swedish Technical Research Board, the A.&L. Grönberg foundation and the K.&A. Wallenberg foundation.

References

Aragón SR, Pecora R (1976) Fluorescence correlation spectroscopy as a probe of molecular dynamics. J Chem Phys 64:1791–1803

Ehrenberg M, Rigler R (1974) Rotational brownian motion and fluorescence intensity fluctuations. Chem Phys 4:390–401

Elson EL, Magde D (1974) Fluorescence correlation spectroscopy. I. Conceptual basis and theory. Biopolymers 13:1–27

Koppel DE (1974) Statistical accuracy in fluorescence correlation spectroscopy. Phys Rev A 10:1938–1945

Koppel DE, Axelrod D, Schlessinger J, Elson EL, Webb WW (1976) Dynamics of fluorescence marker concentration as a probe of mobility. Biophys J 16:1315–1329

Marquardt DW (1963) An algorithm for least-squares estimation of non-linear parameters. J Soc Ind Appl Math 11:431–441

Palmer III AG, Thompson NL (1989) Optical spatial intensity profiles for high order autocorrelation in fluorescence spectroscopy. Appl Opt 28:1214–1220

Qian H, Elson EL (1991) Analysis of confocal laser-microscope optics for 3-D fluorescence correlation spectroscopy. Appl Opt 30:1185–1195

Rigler R, Widengren J (1990) Ultrasensitive detection of single molecules by fluorescence correlation spectroscopy. Bioscience 3:180–183

Rigler R, Mets Ü (1993) Diffusion of single molecules through a Gaussian laser beam. SPIE Proceedings. Laser Applications in Life Sciences. Sept. 1992 Jyväskylä, Finland (in press)

Rigler R, Widengren J, Mets Ü (1992) Interactions and kinetics of single molecules as observed by fluorescence correlation spectroscopy. In: Wolfbeis OS (ed) Fluorescence spectroscopy. New methods and applications. Springer, Berlin Heidelberg New York, pp 13–24

Schneider MB, Webb WW (1981) Measurement of submicron laser beam radii. Appl Opt 20:1382–1388